JOURNAL OF combinatorial CHEMISTRY

Article

High-Throughput Screening and Optimization of Photoembossed Relief Structures

Nico Adams, Berend-Jan De Gans, Dimitri Kozodaev, Carlos Snchez, Cees W. M. Bastiaansen, Dirk J. Broer, and Ulrich S. Schubert

J. Comb. Chem., **2006**, 8 (2), 184-191• DOI: 10.1021/cc0501108 • Publication Date (Web): 15 February 2006

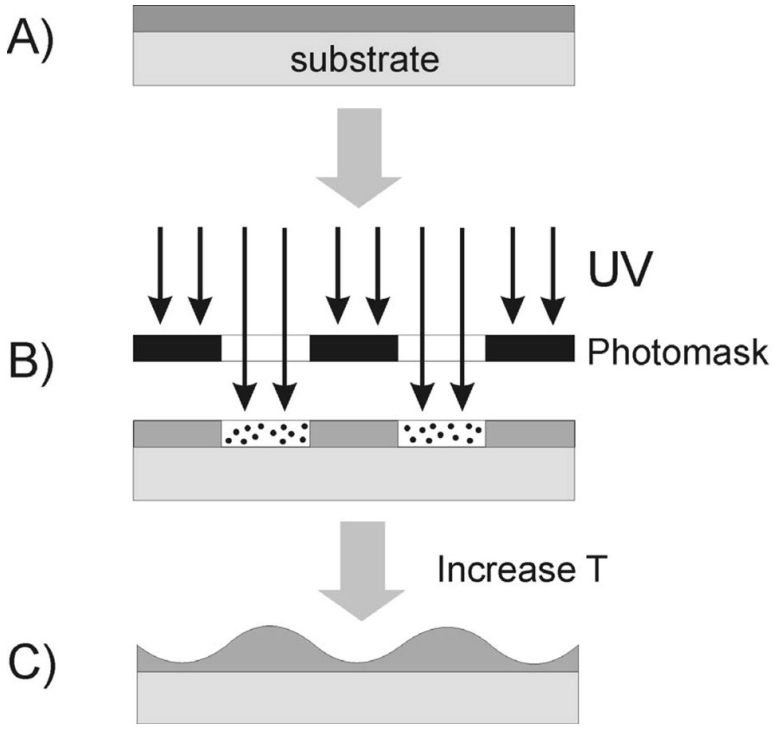

More About This Article

Additional resources and features associated with this article are available within the HTML version:

- Supporting Information
- Links to the 3 articles that cite this article, as of the time of this article download
- Access to high resolution figures
- Links to articles and content related to this article
- Copyright permission to reproduce figures and/or text from this article

Journal of Combinatorial Chemistry is published by the American Chemical Society.
1155 Sixteenth Street N.W., Washington, DC 20036

High-Throughput Screening and Optimization of Photoembossed Relief Structures

Nico Adams,[†] Berend-Jan De Gans,[†] Dimitri Kozodaev,[†] Carlos Sánchez,[‡] Cees W. M. Bastiaansen,[‡] Dirk J. Broer,[‡] and Ulrich S. Schubert*[,†]

Laboratory of Macromolecular Chemistry and Nanoscience, and Polymer Technology Group, Department of Chemical Engineering, Eindhoven University of Technology and Dutch Polymer Institute (DPI), PO Box 513, 5600 MB Eindhoven, The Netherlands

Received August 25, 2005

A methodology for the rapid design, screening, and optimization of coating systems with surface relief structures, using a combination of statistical experimental design, high-throughput experimentation, data mining, and graphical and mathematical optimization routines was developed. The methodology was applied to photopolymers used in photoembossing applications. A library of 72 films was prepared by dispensing a given amount of sample onto a chemically patterned substrate consisting of hydrophilic areas separated by fluorinated hydrophobic barriers. Film composition and film processing conditions were determined using statistical experimental design. The surface topology of the films was characterized by automated AFM. Subsequently, models explaining the dependence of surface topologies on sample composition and processing parameters were developed and used for screening a virtual 4000-membered in silico library of photopolymer lacquers. Simple graphical optimization or Pareto algorithms were subsequently used to find an ensemble of formulations, which were optimal with respect to a predefined set of properties, such as aspect ratio and shape of the relief structures.

Introduction

When compared to classical lithographic[1,2] or mechanical embossing techniques,[3] photoembossing offers a new, versatile, and simple alternative for the production of large-scale/large-area relief structures in thin polymer films.[4−7] Photoembossed substrates find wide applications in technologically diverse areas, but mainly in display technology.[8] A typical photoembossing procedure is a simple and straightforward process in comparison to, for instance, conventional lithography. In the first instance, a substrate is coated with a lacquer composed of a polymeric binder (typically a polyacrylate), a multifunctional monomer, and a photoinitiator. After coating, a mask with a defined grating size is applied, and the coating is irradiated. This results in the generation of a latent image of the mask in the form of free radicals in the coating. Diffusion of the radicals throughout the coating, resulting in blurring or the destruction of the image, is prevented by the glassy nature of the coating. Relief structures are finally created by baking the coating at temperatures above the glass transition temperature (T_g) of the lacquer. Polymerization occurs selectively in the irradiated areas of the lacquer, and the consumption of monomer leads to a net flux of unreacted monomeric material from the nonirradiated areas to the irradiated ones. Such a diffusion is made possible by the increased mobility of the entities enclosed in the polymer matrix by baking. The exposed regions swell and subsequently give rise to the desired relief structures (Figure 1).[9,10] The successful preparation of regular and well-defined relief structures is critically dependent on a number of factors, such as lacquer composition, mask period, exposure times and energies, and baking temperatures and times.

In a previous paper, we have shown how combinatorial and high-throughput techniques can be used to investigate the influence of all of these variables on the surface topology using both gradient and continuous libraries.[11] However, factors were mainly investigated using the one-at-a-time variational principle; i.e., one factor was varied across the library, with the others being kept constant. Although the use of gradients allows the generation of a large number of samples of different compositions in relatively short periods of time, their gradient nature also implies a high screening effort, particularly if the screening resolution is high. Discrete libraries are generally less compositionally diverse, with the consequence that a large number of samples has to be synthesized if a high resolution is desired. Whereas a one-factor-at-a-time strategy enables the experimentalist to understand the fundamental role that each of the investigated parameters plays within a given system, this approach necessarily results in a large number of experiments and will not identify unknown synergies that may exist between several factors. In the previous paper, a total of 220 experiments was carried out, of which 132 experiments concerned the investigation and optimization of factors that will be addressed in the present study.[11]

* To whom correspondence should be addressed. Fax: 0031 40 247 4186. E-mail: u.s.schubert@tue.nl.
[†] Laboratory of Macromolecular Chemistry and Nanoscience.
[‡] Polymer Technology Group.

10.1021/cc0501108 CCC: $33.50
Published on Web 02/15/2006

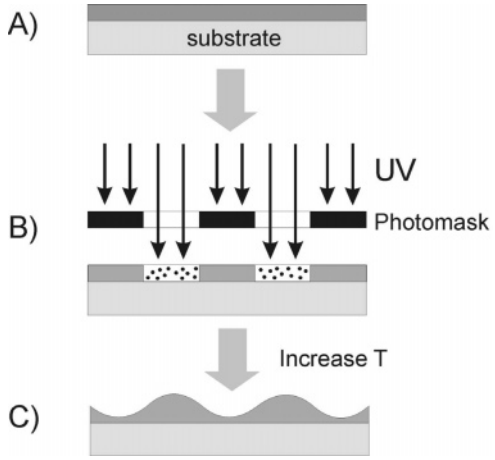

Figure 1. (A) A film is casted on a substrate and (B) subsequently exposed to UV irradiation using a mask of defined grating size, thereby forming a latent image of free radicals entrapped in the polymer matrix. Heating the sample (C) results in local polymerization of the monomer, resulting in a diffusive flux of unreacted monomer toward the exposed regions, which in turn gives rise to a relief structure.

In this paper, we therefore aim to demonstrate how statistical design of experiments coupled with extensive modeling can be used to (a) drastically reduce the number of experiments that need to be carried out, (b) screen virtual formulations, and (c) optimize formulation composition and processing parameters. This is part of an ongoing strategy pursued in the Dutch Polymer Institute's High-Throughput Experimentation Cluster, which focuses on the development of knowledge-based design strategies and the use of predictive technologies for a more focused approach to high-throughput experimentation.[12]

Experimental Section

Materials. Polybenzyl methacrylate (M_w 70 kD; Scientific Polymer Products) was used as binder, dipentaerythritol penta/hexaacrylate (Sigma-Aldrich, Steinheim, Germany) as multifunctional monomer, and Irgacure 369 (Ciba) as photoinitiator. Isopropyl acetate (Acros Organics, Geel, Belgium) and methylbenzoate (Fluka Chemika, Buchs, Switzerland) were used as solvents. Solutions of monomer, binder, and initiator in a 90/10% w/w mixture of isopropyl acetate/methylbenzoate were prepared by gentle stirring. In the past, it was shown that the latter solvent mixture is particularly effective in suppressing ring formation.[13] All solutions contained 4.0 wt % solid material and were filtered through 5-μm PTFE filters (Schleicher & Schuell, Dassel, Germany) before use.

Substrate Preparation. Discrete libraries were prepared using D263 glass plates, thickness 1.1 mm and 127 × 30 mm in size. The size of the glass plates was determined by the size of the lithographic masks that will be discussed later. Glass plates were cleaned by ultrasonication in acetone for 5 min, rubbed with sodium dodecyl sulfate solution, ultrasonicated in sodium dodecyl sulfate solution for 5 min, flushed with demineralized water to remove the soap, ultrasonicated in 2-propanol, dried with an air flow, and subsequently treated in a UV−ozone reactor (PR-100, UVP, Upland, CA) for 30 min to remove any remaining organic contamination.

Immediately after cleaning, the glass plates were spin-coated with a layer of NFR-016D4 negative photoresist (JSR, Tokyo, Japan) at 1000 rpm for 120 s using a Karl Suss RC8 spin-coater. The photoresist was dried on a hotplate at 90 °C for 120 s and exposed to broadband UV light (Philips) for 5 min using a homemade steel mask. The sample was subsequently baked at 90 °C for 5 min and, finally, developed using TMA-238WA developer (JSR, Tokyo, Japan). The substrate was cleaned thoroughly by flushing with demineralized water and subsequently treated in a UV−ozone reactor (PR-100, UVP, Upland, CA) for 30 min. The substrate was then coated with (tridecafluoro-1,1,2,2-tetrahydro-octyl)-trichlorosilane (ABCR, Karlsruhe, Germany).[14] The UV−ozone treatment in this case replaces the treatment with the oxygen plasma. In a final step, the cross-linked photoresist was removed with acetone using ultrasonication. On each of the substrates prepared in this manner, 11 × 4 samples can be deposited. The dried films have a size of 8.5 × 4.3 mm.

Library Preparation. All libraries were prepared under Class 100 clean room conditions. Small volumes of solution (3−13 μL) were deposited manually with a pipet (Brand Transferpette, Wertheim, Germany) onto a chemically patterned substrate and allowed to dry under ambient conditions. Gratings were generated with a USHIO lithographic system (filter at 365 nm) in combination with a rectangular lithographic line mask (101 × 20 mm), which was divided into four sectors (101 × 5 mm). The sectors differ in periodicity of the lines (40, 20, 10, and 5 μm, respectively). The power that reached the sample was 5 mW cm^{-2}. After exposure, the grating was developed for 10 min on a hotplate at 80 °C. Finally, the samples were flood-exposed for 10 min and heated to 80 °C for an additional 10 min to fix the surface relief structure. On the final relief structure, this fixation step has virtually no influence.

Topography Characterization. Atomic force microscopy (AFM) was used for the purpose of topography characterization. A Solver LS (NT-MDT, Russia) instrument with an automated Yθ stage for positioning and a circular workspace with an accessible diameter of 15 cm was used. The maximum scan size is 100 × 100 × 10 μm. In addition, the Solver LS has an integrated optical system with 1.5-μm resolution. Cantilevers with a spring constant of 5.5 N m^{-1} (NSG01, NT-MDT, Russia) were used. All measurements were performed in tapping mode.

To improve the quality of the data, four maximum size scans per film were performed, yielding a total of 44 × 4 = 176 scans per library. Scans were situated at the edges of a 1 × 1 mm square, in the middle of the film. To reduce the effect of scanner nonlinearity, the measuring time per scan was at least 3 min; the total measuring time per library was, therefore, ∼9 h. The roughness was analyzed with the aid of integrated software tools based on the set of statistic equations according to ISO4287/1 standard.

Computational Procedure. Design of experiments, data analysis and optimization procedures were carried out using the MS FAST package by Accelrys.[15] Data visualization and

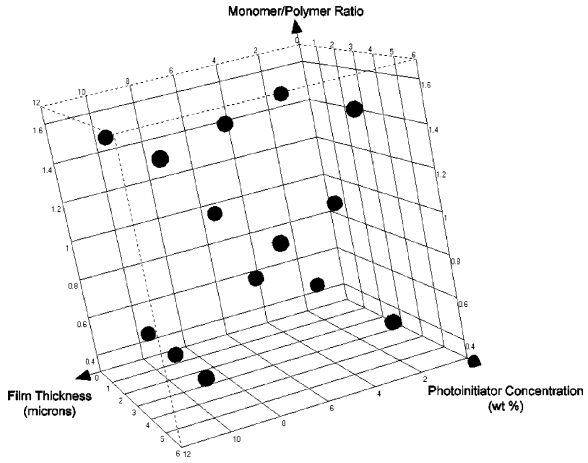

Figure 2. Candidate points in design space.

visual optimization were carried out using the Spotfire Decision Site package.[16] Because the number of experiments that could be carried out was limited due to the complexity of the sample preparation and the time available for the execution of the project, a D-optimal design (quadratic model) was chosen. Design factors include the photoinitiator concentration (range 1−5%), the monomer-to-binder ratio (range 0.5−1.5), and the thickness of the coating (range 2−10 μm). Because the ultimate goal of the design of experiment exercise is the optimization of film surface topologies (i.e., maximum relief height and shape factor), a response surface design was required. The response variables were the relief height and the shape factor. Although the relief height is a straightforward property measure of the photoembossed structures and defined as the difference in height between the medium parts of the irradiated and the dark areas, the quantitative representation of the changing film shapes of the photoembossed structures is not trivial. In an attempt to assign a scalar measure to the shape of the relief structure, we applied a Fourier analysis approach that leads to a "shape factor" (S), which is independent of the relief height and the grating period. In a first step, the atomic force microscope data were processed in such a way as to produce an average one-dimensional surface curve $f(x)$. Second, the first few Fourier series coefficients,

$$a_m = \Lambda^{-1} \int f(x) e^{-(i2\pi mx/\Lambda)}\, dx \qquad (1)$$

(where the integral occurs over one period) were determined. Finally, a shape factor defined as

$$S = \frac{|a_1|^2 - \sum_{n=2}^{M} |a_n|^2}{\sum_{n=1}^{M} |a_n|^2} \qquad (2)$$

where M, the maximum number of coefficients used for the calculation, was computed (in practice we let $M = 5$, since the higher Fourier terms were all nearly 0 for all the topologies in our samples). The shape factor, S, was inspired by the Michelson contrast,[17] used in image processing and information displays, and has the following properties: surface relief profiles very similar to a sinusoid will lead to a value close to +1, whereas a lower value indicates deviation of the shape from a sinusoid. A value close to −1 typically indicates the strong appearance of the shoulders at the edge of the relief plateaus (which are higher-order spatial frequencies). A value of 0.73 corresponds to an approximately square shape, that is, a block wave.

Models were developed using the genetic function approximation tools implemented in MS FAST.[15] Pareto optimizations were carried out using an optimization algorithm also implemented in MS FAST.

Results and Discussion

Library Design and Screening Results. To investigate the response surface associated with the experimental factors

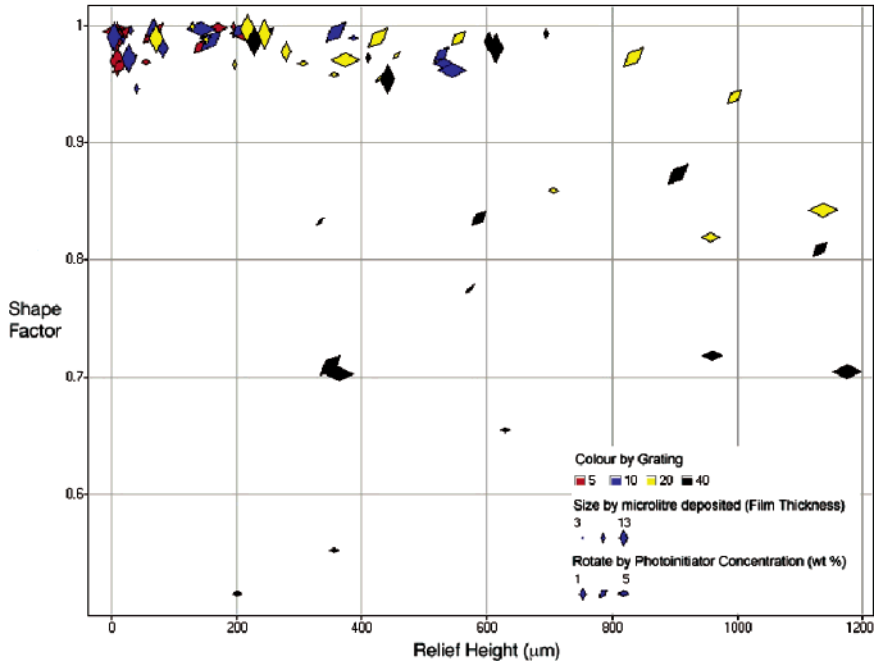

Figure 3. Experimental screening data.

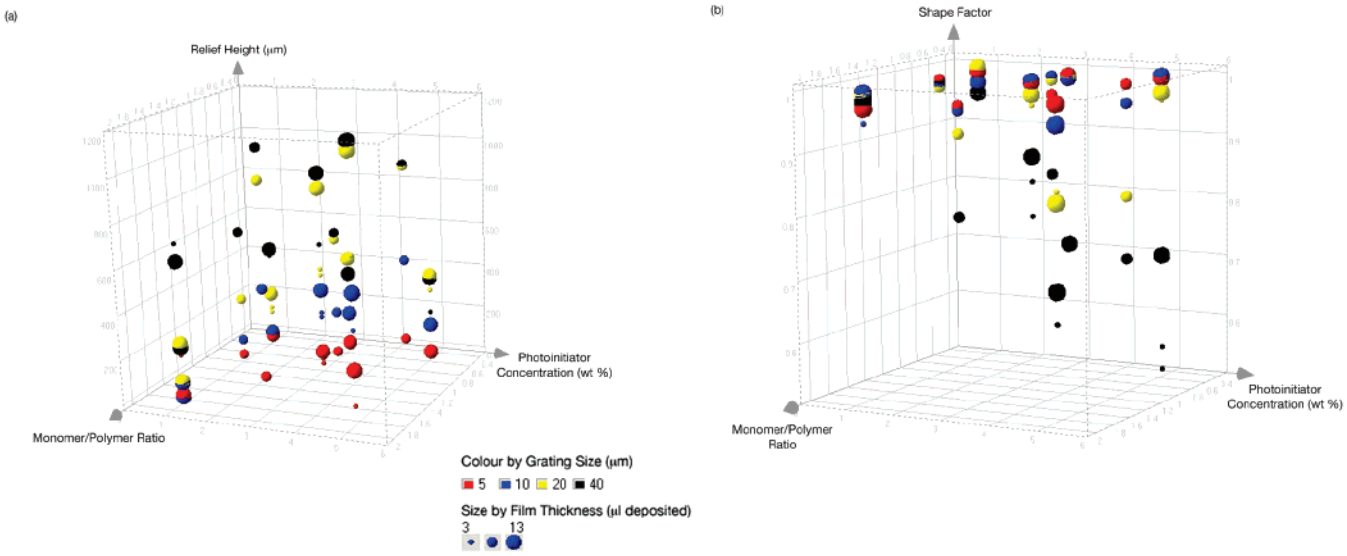

Figure 4. Influence of the experimental factors on the (a) relief height and (b) shape factor.

monomer/polymer ratio (0.5−1.5), film thickness (2−10 μm), and photoinitiator concentration (1−5 wt %), a D-optimal design (quadratic model) was chosen. Within the specified constraints, this led to 18 candidate points (Figure 2), including lack-of-fit and replicate points. These were subsequently replicated over four different grating sizes (5, 10, 20, and 40 μm), resulting in 72 datapoints in total. Due to experimental expediency, the grating sizes were not treated as a design factor.

Once prepared, the photoembossed structures were characterized by their relief height and shape factor. When examining the data, a number of observations can be made (Figure 3). First and foremost, it can be seen that high relief heights preclude high shape factors and vice versa. Any "optimized" lacquer formulation, in which the optimality criterion involves both maximizing the relief height as well as the shape factor will, therefore, necessarily be a compromise solution. This is supported by the observation that high relief heights are achieved using large grating sizes (predominantly between 20 and 40 μm) and medium to large amounts of photoinitiator, as well as large film thickness, whereas high shape factors and, therefore, sinusoidal patterns are more frequently achieved using smaller pitches and small amounts of photoinitiator (Figure 4a, b). There is no significant correlation between the shape factor and the film thickness.

These observations are consistent with previous experience. In the past, we have been able to show that, whereas sinusoidal surfaces can be achieved with small grating sizes, the use of 20- and 40-μm gratings leads to shoulder formation at the edges of the irradiated area and, therefore, to a lowering of both the shape factor (deviation from sinusoidal shape) and the relief height (Figure 5).[11] This phenomenon can be explained by overexposure of the lacquer: excessive cross-linking as a consequence of radical-induced polymerization prevents unreacted monomer from diffusing into the center of the exposed surface. Instead, monomer accumulates at the edges, forming shoulders. Qualitatively, the screening data also confirm some of the other observations made in the one-variable-at-a-time experiments: it could be shown,

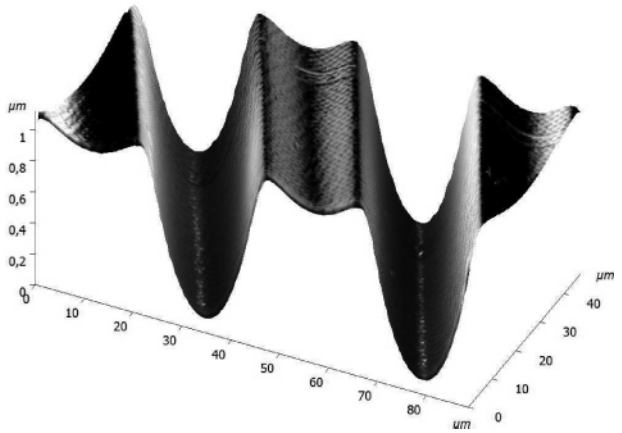

Figure 5. Deviation from a sinusoidal shape of a photoembossed surface, prepared using a 40-μm grating.

for example, that neither relief height nor shape factor vary as a function of grating size below a certain threshold. Furthermore, clear dependencies of the relief height on the monomer-to-polymer ratio and photoinitiator concentration can be observed, which are, however, more complex than the data from the one-variable-at-a-time screening would suggest.

Model Development. Models accounting for the dependence of the two response variables on the experimental factors were developed using genetic function approximation (GFA) techniques.

Genetic function approximation uses genetic algorithms (GA) to determine the most important factors in a dataset and subsequently uses these for the development of linear least squares regression models. The method works by coding regions in parameter space, which are to be searched, into strings. An ensemble of strings is called a population. Once this has been done, selection, crossover, and mutation operations are performed, and members which have been newly added to an equation are scored using a predefined measure of fitness, which is usually related to the fit of the prediction with the observed data. The procedure will be continued until a calculation converges or it reaches a user-defined limit of cycles. To guard against overfitting, the

Table 1. Regression Equations and Validation Data Returned by the Genetic Function Approximation Procedure[a]

	equation	R^2	$R^2_{adjusted}$	$R^2_{cross-validated}$	significance of regression F value
1	$RH = -344 + 43.20(GS) - 0.63(GS)^2 + 61.90(PI)(MP)$	0.689	0.676	0.640	53
2	$RH = -703 + 119.00(FT) + 43.20(GS) - 6.93(FT)^2 - 0.63(GS)^2 + 59.50(PI)(MP)$	0.755	0.738	0.702	43
3	$RH = -131 + 14.10(GS) + 61.90(PI)(MP)$	0.626	0.615	0.581	61
4	$S = 0.921 + 0.022(PI) + 0.009(GS) - 0.0001(GS)^2 - 0.003(PI)(GS)$	0.883	0.876	0.859	133
5	$S = 103 - 0.0002(PI)(GS)$	0.819	0.816	0.799	334
6	$S = 0.967 + 0.022(PI) + 0.002(GS) - 0.003(PI)(GS)$	0.859	0.852	0.836	145

[a] RH = relief height; S = shape factor; GS = grating size; PI = photoinitiator concentration (wt %); MP = monomer/polymer ratio; FT = film thickness (measured as the amount of lacquer solution deposited (in μL)

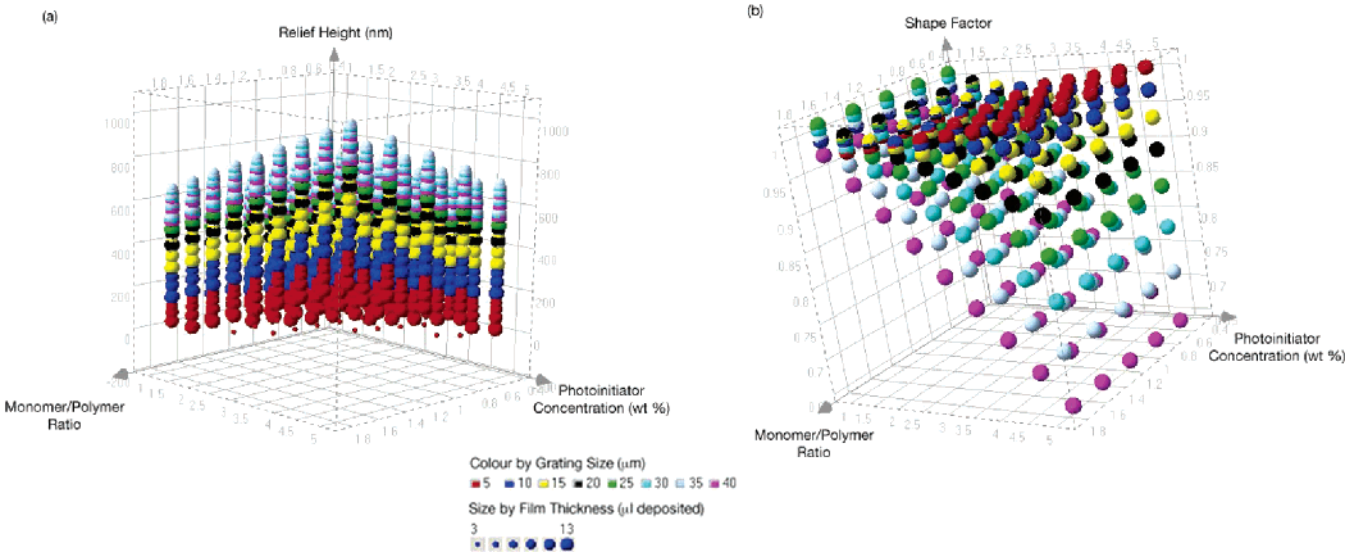

Figure 6. In silico screening of virtual photoembossing formulations using regression models 2 and 4.

equations were scored using the Friedman lack-of-fit score, which actively penalizes equations with large sum-of-squares errors and large numbers of independent variables.[18]

The top three equations for both relief height and shape factor resulting from the genetic function approximation are given in Table 1. Models perform adequately, and the fact that R^2, $R^2_{adjusted}$, and $R^2_{cross-validated}$ have very similar values suggests that the models are stable. It can be seen that the relief height is crucially dependent on the grating size, the photoinitiator concentration, and the monomer-to-polymer ratio. One model also seems to imply an influence of the film thickness on the relief height. A quadratic interaction between photoinitiator concentration and monomer to polymer mass ratio is clearly observed, which accounts for the influence of reaction kinetics on the final relief height. Again, this is consistent with previous experience, because it could be demonstrated that the relief height is dependent on all of these variables except for the film thickness: single-factor experiments seem to suggest that there is only a relationship between relief heights and film thickness, if large grating sizes (20 or 40 μm) are used. Therefore, this factor is clearly less important in determining the relief height and appears less frequently in the regression models. In terms of the shape factor, all models agree that only the photoinitiator concentration and the grating size are of importance. Again, this is consistent with prior experience: large grating sizes lead to deviation from the desired sinusoidal shape due to the potential for overexposure (see above). The photoinitiator concentration is correlated to the degree of cross-linking in the lacquers and, therefore, to the ability of unreacted monomer to diffuse and build up the desired structures, which will, again, lead to deviations from sinusoidal shapes.

Virtual Screening and Optimization. To investigate the whole response surface associated with the experimental factors and the grating size, we constructed ~4000 virtual formulations through systematic variation of the factors within the upper and lower validity limits of the regression models. Subsequently, relief heights and shape factors were predicted using models 2 and 4. The results are shown in Figure 6. Such a procedure produces a relatively fine-grained response surface, which serves to confirm some of the previous observations (Figure 7). The curved nature of the surface makes it much easier to see how high shape factors and large relief heights seem, to a certain degree, to be mutually exclusive.

Due to the very fine-grained nature of the surface, it is possible to perform a simple optimization-by-filtering given a set of defined performance criteria. This removes all of those formulations that do not conform to the predefined criteria. Formulations that remain are "optimal" solutions with respect to predefined property/performance criteria. For the purposes of this study, this meant trying to maximize both the shape factor and the relief height at low grating sizes. In numerical terms, formulations with shape factors

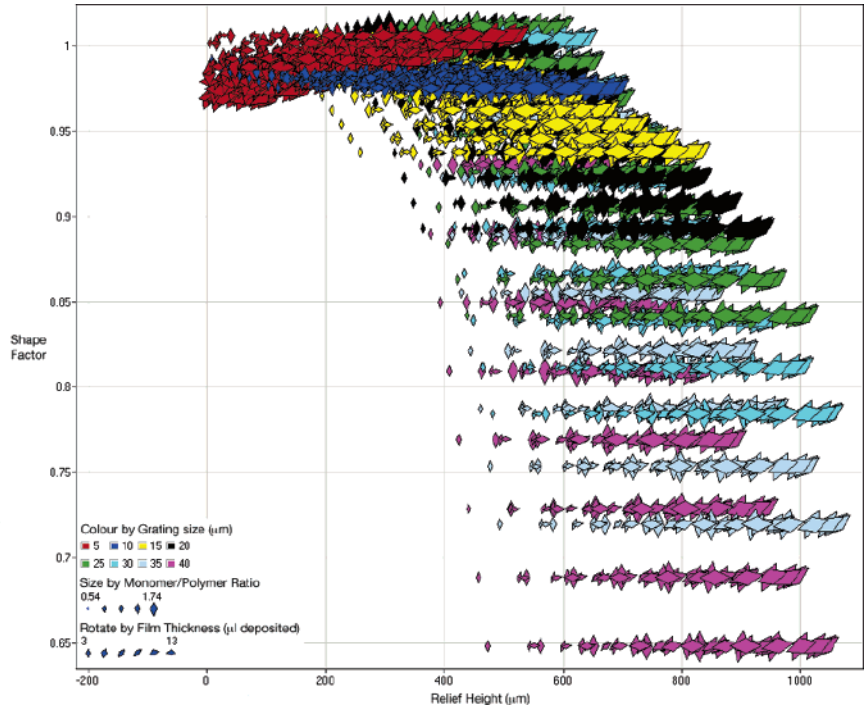

Figure 7. Relief height vs. shape factor for virtual formulations based on predictions by regression models 2 and 4.

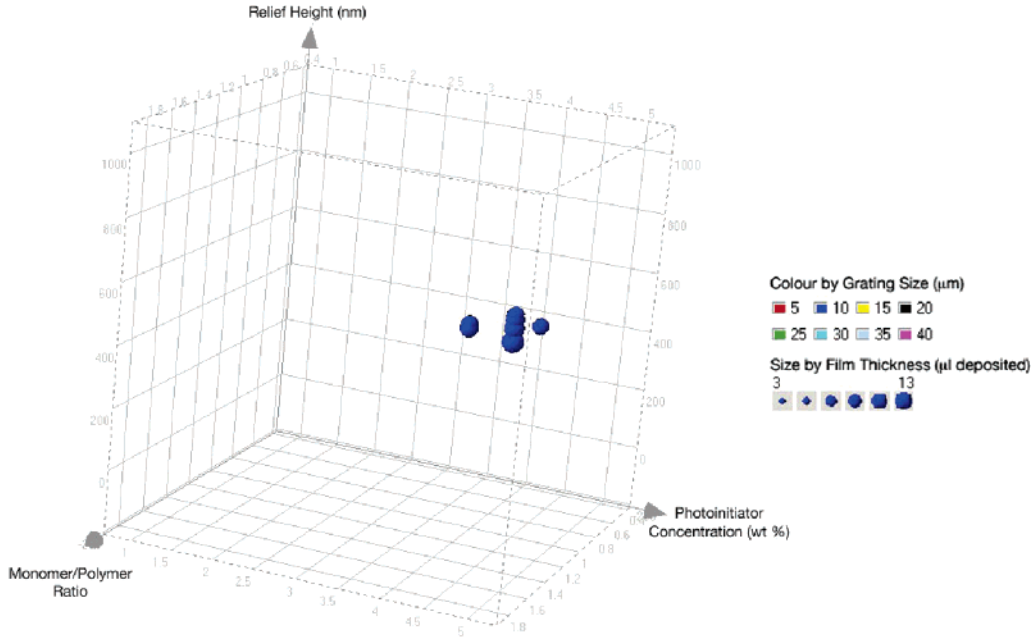

Figure 8. Optimized solutions resulting from "graphical optimization."

higher than 0.95, relief heights in excess of 600 nanometers, and produced using grating sizes ≤10 μm were considered to be "optimal". Multicriteria filtering gave a small set of optimal solutions, which conform to all of these requirements (Figure 8). All solutions fall within a narrow composition and processing parameter range and can, for practical purposes, be considered to be identical (Table 2). To achieve both high shape factors and relief heights, high photoinitiator concentrations (5 wt %), medium to large film thicknesses (8−13 μL), and high monomer-to-polymer mass ratios (1.86) are required when using gratings of 10 μm. Gratings of 5-μm size lead to predicted relief heights of ∼505−520 nm (±60 nm). The physical rationalization of these results probably consists of a combination of mutually reinforcing effects, consistent with previous experience. In the past, it could be shown that small grating sizes of 5 and 10 μm are conducive to achieving high shape factors by avoiding "overexposure" and, therefore, shoulder formation.[11] High amounts of photoinitiator concentrations in the system will lead to the generation of a large number of radicals upon exposure to light. When coupled with a high monomer-to-polymer ratio (i.e., a high concentration of reactive monomer), this will

Table 2. Optimized Photoembossing Formulations Using a Graphical Optimization Procedure

				relief height		shape factor	
photoinitiator concn (wt %)	grating size (μm)	film thickness (μL deposited)	monomer/polymer ratio	predicted (nm)	predicted estimation error (nm)	predicted	estimation error
4.5	10	7	1.74	623.1	51.7	0.977	0.007
4.5	10	8	1.74	637.9	52.6	0.977	0.007
4.5	10	9	1.74	638.8	51.6	0.977	0.007
4.5	10	10	1.74	625.8	49.1	0.977	0.007
5	10	5	1.74	603.9	50.8	0.975	0.008
5	10	6	1.74	646.3	53.6	0.975	0.008
5	10	7	1.74	674.9	55.8	0.975	0.008
5	10	8	1.44	600.4	49.9	0.975	0.008
5	10	8	1.74	689.7	56.7	0.975	0.008
5	10	9	1.44	601.3	48.9	0.975	0.008
5	10	9	1.74	690.6	55.8	0.975	0.008
5	10	10	1.74	677.6	53.6	0.975	0.008
5	10	11	1.74	650.8	50.9	0.975	0.008
5	10	12	1.74	610.1	49.8	0.975	0.008

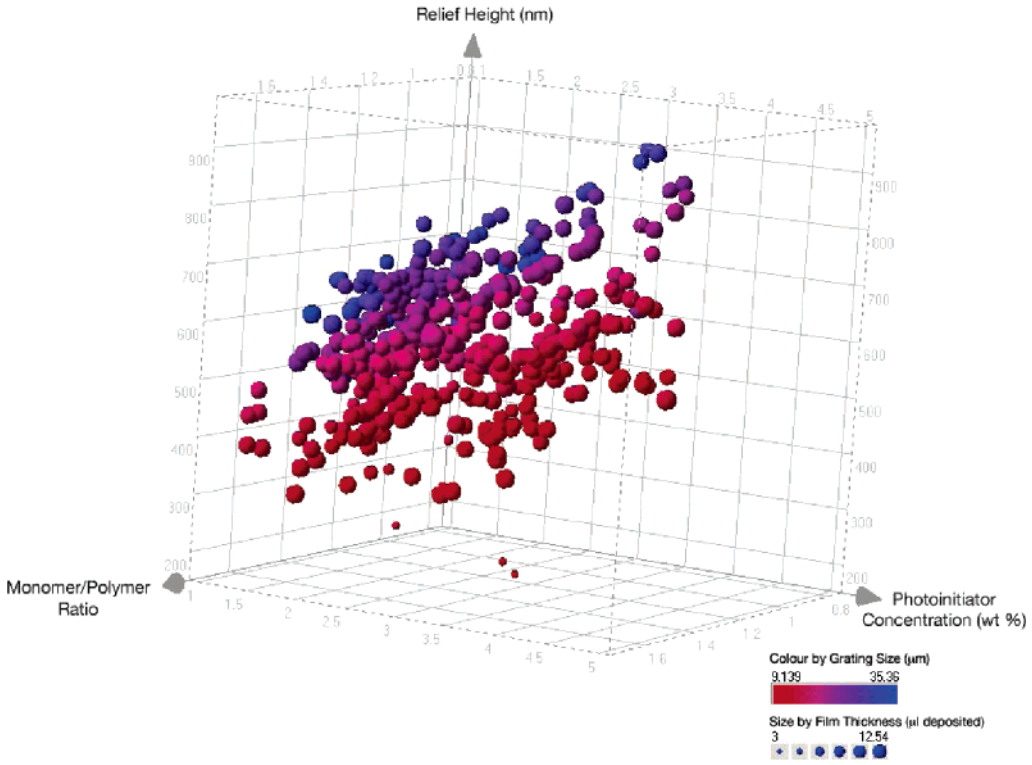

Figure 9. Pareto-optimal surface for photoembossing lacquers.

ensure a high cross-linking density as well as a sufficient flux of unreacted material. Both of these phenomena will be crucial in attaining a satisfactory relief height.

Tradeoff or "Pareto" optimization is an alternative approach to finding optimal solutions. During a Pareto optimization, multiple properties of a system are simultaneously optimized, without disadvantaging any single property in the process. For a two-dimensional space, such solutions fall on a curve; for an *n*-dimensional space, points would be located on an $n-1$-dimensional surface. Points on a Pareto-optimal surface/curve have the best possible combination of properties, whereas for all other points in space, there is at least one point on the surface which is as good or better in terms of properties or performance. Figure 9 shows all possible Pareto-optimal solutions for the present system within the validity constraints of models 2 and 4. Optimizer targets were to maximize both relief height and shape factor. Again, a simple filtering operation can now be used to find those points on the Pareto surface that fulfill predefined criteria, such as grating size and shape factor. The best solution found in this way is a formulation consisting of 4.64 wt % photoinitiator, a monomer/polymer ratio of 1.47, a film thickness of 10 (μL deposited), and irradiated using a 10-μm grating. The predicted relief height is 570 nm ($\pm$45 nm) with a shape factor of 0.977 ($\pm$0.008). The results show that, in this case, Pareto optimization and simple optimization-by-filtering give similar results, given a set of common constraints.

Experimental Verification. To confirm the optimized solutions as "hits", control experiments would normally be carried out at this stage. However, upon reexamination of the screening data, we have found that some of the candidate

Table 3. Screening Data Close to Optimal Solutions

photoinitiator concn (wt %)	grating size (μm)	film thickness (μL deposited)	monomer/polymer ratio	relief height (nm)	relief height error (nm)	shape factor	shape factor error
5	10	13	1.86	544	16	0.96	0.02
5	10	8	1	530	66	0.96	0.01
3	10	8	1.86	526	10	0.97	0.02

points in the original experimental design already come extremely close to optimal solutions predicted by graphical or Pareto methods (Table 2, Table 3). Graphical optimization predicts a formulation consisting of 5 wt % of photoinitiator, a monomer/polymer ratio of 1.44, and a "film thickness" of 8 μL deposited and irradiated using a 10-μm grating to have a relief height of 600.4 nm ($\pm$49.9 nm) and a shape factor of 0.975 ($\pm$0.008). One of the screening candidate points showed a relief height of 530 nm ($\pm$66 nm) and a shape factor of 0.96 ($\pm$0.001) for a composition, which differs only in the monomer/polymer ratio, with the screening point having a value of 1, as opposed to 1.44 for the virtual formulation. Taking into account the estimated prediction as well as the relatively large measurement errors, it is believed that these results are in good agreement. Furthermore, we showed in a previous publication that small differences in composition or processing conditions, such as those observed between the predicted "optimal" points and the experimentally evaluated points, will not have a significant effect on either relief height or shape factor.[11] The predictions are, therefore, considered validated by already existing screening data, and further experimental investigations (which would, in effect, only be repeating experiments which have already been performed) were deemed unnecessary. However, it is important to stress that this is purely accidental. Had the optimal criteria been different and the definition of "optimal" been far away from the design points, experimental verification would be mandatory.

Summary and Conclusions

A complete workflow for the rapid investigation and optimization of photopolymer lacquers for photoembossing applications, based on a combination of rational library design and data-mining, combined with high-throughput synthesis and screening techniques, was developed. Using D-optimal design, a library of 72 rectangular films was developed by dispensing a given amount of sample on a chemically patterned substrate consisting of hydrophilic areas separated by fluorinated hydrophobic boundaries. After appropriate processing, the films were screened with respect to their surface topography (relief height and shape factor). Subsequently, models explaining the observed relief height and shape factor as a function of film composition and processing conditions were built. Model development was carried out using genetic function approximation. The models indicate that the observed relief heights are dependent on all of the investigated variables (photoinitiator concentration, monomer-to-polymer ratio, grating size, and film thickness), whereas the shape factor only shows a dependence on the photoinitiator concentration and the grating size. Subsequently, these models were used to predict the surface topographies of $\sim$4000 virtual formulations, which could thus be screened in silico. The resulting fine-grained response surface was used to find ensembles of formulations, which are optimal with respect to a predefined set of performance criteria (maximize relief height, shape factor > 0.95, grating sizes not larger than 10 μm) using a simple, graphical optimization procedure. In an alternative optimization approach, a Pareto algorithm was used, which, once the above constraints were applied, allowed us to come to the same conclusions as the simple graphical optimization.

It was demonstrated that a combination of experimental design, high-throughput experimentation, and virtual screening and optimization can significantly reduce the number of experiments that need to be carried out during a discovery and optimization campaign, leading to more efficient R&D and, in a commercial context, ultimately to faster product development.

Acknowledgment. The authors acknowledge the Dutch Polymer Institute (Project no. 500), NOW, and the Fonds der Chemischen Industrie for financial support of this work.

References and Notes

(1) Chou, S. Y.; Krauss, P. R.; Zhang, W.; Guo, L.; Zhuang, L. *J. Vac. Sci. Technol., B* **1997**, *15*, 2897.
(2) Chou, S. Y.; Krauss, P. R. *Microelectron. Eng.* **1997**, *35*, 237.
(3) Heckele, M.; Bacher, W.; Mueller, K. D. *Microsyst. Technol.* **1998**, *4*, 122.
(4) Croutxé-Barghorn, C.; Lougnot, D. J. *J. Pure Appl. Opt.* **1996**, *5*, 811.
(5) Sakhno, O.; Smirnova, T. *Optik* **2002**, *113*, 130.
(6) Witz, C.; Sánchez, C.; Bastiaansen, C. W. M.; Broer, D. J. In *Handbook of Polymer Reaction Engineering*; Meyer, T., Keurentjes, J., Eds.; Wiley-VCH: Weinheim, 2005; Vol. 19.
(7) De Witz, C.; Broer, D. J. *Polym. Preprints* **2003**, *44*, 236.
(8) http://www.research.philips.com/technologies/light_dev_microsys/selforgpol/
(9) Leewis, C. M.; De Jong, A. M.; van IJzendoorn, L. J.; Broer, D. J. *J. Appl. Phys.* **2004**, *95*, 4125.
(10) Leewis, C. M.; De Jong, A. M.; van IJzendoorn, L. J.; Broer, D. J. *J. Appl. Phys.* **2004**, *95*, 8352.
(11) De Gans, B.-J.; Sanchez, C.; Kozodaev, D.; Alexeev, A.; Escuti, M.; Bastiaansen, C. W. M.; Broer, D. J.; Schubert, U. S. **2005**, submitted.
(12) Adams, N.; Schubert, U. S. *QSAR Comb. Sci.* **2005**, *24*, 58.
(13) Tekin, E.; De Gans, B.-J.; Schubert, U. S. *J. Mater. Chem.* **2004**, *14*, 2627.
(14) Trimbach, D.; Feldman, K.; Spencer, N. D.; Broer, D. J.; Bastiaansen, C. W. M. *Langmuir* **2003**, *19*, 10957.
(15) Accelrys. *MS FAST Documentation*; 2005.
(16) http://www.spotfire.com
(17) Bex, P.; Makous, W. *J. Opt. Soc. Am. A* **2002**, *19*, 1996.
(18) Friedman, J. H. *Multivariate Adaptive Regression Splines*; Technical Report No. 102; Laboratory for Computational Statistics, Department of Statistics, Stanford University: Stanford, CA, 1990.

CC0501108